

Theoretical and Experimental Evaluation of Transmission Loss of Cylinders

Yiren S. Wang,* Malcolm J. Crocker,† and P. K. Raju‡
Purdue University, West Lafayette, Indiana

A light aircraft fuselage was idealized by a cylindrical shell. Its sound transmission loss was evaluated theoretically by using statistical energy analysis (SEA). The parameters used in SEA were obtained theoretically from the wavenumber diagrams using a computer. Experimentally, the incident sound intensity was measured with a single microphone and by making an assumption about the sound field. The transmitted sound intensity was measured using the new two-microphone acoustic intensity technique with the aid of a fast Fourier transform analyzer. The results obtained from the theoretical SEA model for the sound transmission loss compared well with the experimental result.

I. Introduction

DURING recent years, there has been a growing interest in the interior noise levels of general aviation aircraft. The noise is associated primarily with sources such as the propellers, the engines, and the engine exhausts. Studies of general aviation aircraft have indicated that the noise is transmitted into the interior through airborne and structure-borne paths. At the same time, there has been an increasing demand on the general aviation industry to reduce the cabin noise levels. Hence, it is important to study the noise transmission characteristics of such aircraft structures.

The sound transmission properties of a structure may be evaluated from a knowledge of its transmission loss, which is a function of the ratio of the incident sound power to the transmitted sound power. Hence, development of both accurate prediction and measurement techniques for the evaluation of the transmission loss of structures is very important in the study of sound transmission through fuselage walls. In this paper, the fuselage structure has been idealized into a cylindrical shell. The dimensions of the cylinder were chosen to simulate a half-scale model of a light aircraft fuselage. The transmission loss was estimated theoretically by using principles of statistical energy analysis (SEA). The parameters involved in the SEA model, such as modal densities and radiation efficiencies, were obtained from the wavenumber diagrams.

The sound transmission loss of the structure was measured experimentally using a newly developed method. This new method has been developed using direct measurements of the intensity transmitted through a structure using the acoustic intensity technique. The incident intensity is obtained through the measurement of the diffuse field intensity in the transmission room or air space. Two cases have been studied. In the first case, the sound source was located inside the cylinder which was placed in an anechoic room. The interior sound field is assumed to be diffuse. In the second case, the source was outside the cylinder which was placed in a reverberation room. In this second case, the interior of the cylinder was

filled with fiberglass making it anechoic. In both the cases, the transmitted intensity in the receiving space was measured using the two-microphone acoustic intensity technique. Thus, in these two cases studied, the transmitting space was assumed reverberant and the receiving space anechoic. The experimental results compared fairly well with the theoretical predictions made from the SEA model.

II. Theoretical Analysis

Instead of solving for the response of each mode individually, SEA investigates the average behavior of variables over a frequency band. Among the most essential parameters in the SEA model are the modal density, mode classification (surface modes, edge modes, and corner modes), and loss factors. All these parameters may be obtained from the wavenumber diagrams. One other important parameter, namely, the damping loss factor of the structure, usually must be obtained experimentally.

Natural Frequencies of a Cylindrical Shell

The natural frequencies of a uniform cylindrical shell can be obtained from Love's equation.¹ When the transverse vibration is considered exclusively, the formula to calculate the natural frequencies can be largely simplified using some practical assumptions. The simplified equations are known as the Donnell-Mushtari-Vlasov equations.² Soedel³ recently modified the formula for the natural frequencies to give the following form:

$$\omega_{mn} = \left\{ \frac{Eh\eta_m^4}{R^2L^4[(n^2/R^2) + (\eta_m^2/L^2)]^2} + D \left(\frac{n^2}{R^2} + \frac{\eta_m^2}{L^2} \right)^2 \right\}^{1/2} \left[\frac{1}{\rho_m h} \right]^{1/2} \quad (1)$$

where ω_{mn} is the angular frequency of the m, n mode, E Young's modulus, h the thickness, R and L the radius and the length of the cylinder, respectively, D the bending stiffness, ρ_m the mass density of the material, and η_m the root of the analogous beam equation.

For the case of simply-supported boundary conditions at both ends of the cylinder, the preceding formula can be reduced to

$$\omega_{mn} = \frac{1}{R} \left\{ \frac{(m\pi R/L)^4}{(m\pi R/L)^2 + n^2} + \frac{(h/R)^2}{12(1-\mu^2)} \right\}^{1/2} \left[\frac{E}{\rho_m} \right]^{1/2} \times \left[\left(\frac{m\pi R}{L} \right)^2 + n^2 \right]^{1/2} \left[\frac{E}{\rho_m} \right]^{1/2} \quad (2)$$

Presented as Paper 81-1971 at the AIAA 7th Aeroacoustics Conference, Palo Alto, Calif., Oct. 5-7, 1981; submitted Oct. 16, 1981; revision received May 7, 1982. Copyright © American Institute of Aeronautics and Astronautics, Inc., 1982. All rights reserved.

*Graduate Research Assistant, Ray W. Herrick Laboratories, School of Mechanical Engineering.

†Professor of Mechanical Engineering, Assistant Director of the Ray W. Herrick Laboratories, Acoustics & Noise Control, School of Mechanical Engineering.

‡Visiting Professor, on leave from Jawaharlal Nehru Technological University, College of Engineering, Kakinada, India.

where μ is Poisson's ratio. In Eqs. (1) and (2), the term η_m , which is the root of the analogous beam equation, can be determined for a given boundary condition. Knowing the value of η_m for a given boundary condition, the natural frequencies of a cylinder may be determined from Eq. (1). This is illustrated in Fig. 1 for two cases: 1) simply-supported and 2) clamped-clamped boundary conditions for a cylinder. It is observed from Fig. 1 that the effect of changing the boundary conditions on the natural frequency of the cylinder is less for the higher-order mode numbers. Hence, the boundary conditions of the cylinder under investigation are assumed to be simply supported even though they may be nearer to the clamped-clamped case.

Wavenumber Diagrams of a Cylinder

The wavenumber diagram (sometimes called the "k-space diagram") has been found to be a very powerful tool in SEA. The wavenumber functions are defined as⁴

$$k_a = (m\pi/L) [h^2 R^2 / 12(1-\mu^2)]^{1/4} \quad (3)$$

$$k_c = (n/R) [h^2 R^2 / 12(1-\mu^2)]^{1/4} \quad (4)$$

where k_a and k_c are the longitudinal wavenumber and circumferential wavenumber functions, respectively. The advantage of using the wavenumber functions rather than frequencies is that Eq. (2) can be simplified further into the following form:

$$\omega_{mn} = [(k_a^2 + k_c^2)^2 + k_a^4 / (k_a^2 + k_c^2)^2]^{1/2} 2\pi f_r \quad (5)$$

where f_r is the ring frequency of the cylinder

$$f_r = \left(\frac{1}{2\pi R} \right) \sqrt{\frac{E}{\rho_m}}$$

Equation (5) can be plotted as k_a vs k_c , for a given frequency. The resulting plot is known as the wavenumber diagram. Figure 2 shows a wavenumber diagram for five normalized frequencies $\nu_0 = 0.4, 1.0, 1.6, 3.2$, and 4.0 , where $\nu_0 = \omega_{mn} / 2\pi f_r$. Also shown in the same figure is the corresponding acoustic wavenumber k as segments of a circle with radii of $\nu_0 \sqrt{f_r / f_c}$.

Acoustically Fast and Slow Modes

Acoustically fast modes of a cylinder are defined as the modes for which both the longitudinal wavenumber and the circumferential wavenumber are less than the corresponding acoustic wavenumber. These modes play a key role in the sound radiation. The acoustically slow modes are those modes for which either the longitudinal wavenumber k_a and/or the circumferential wavenumber k_c are larger than the corresponding acoustical wavenumber k . Following these definitions, the modes on the wavenumber diagram can be classified easily as either acoustically fast or acoustically slow as shown in Fig. 3.

Radiation Efficiency

The radiation efficiency indicates how efficiently sound is radiated from a structure to the acoustic field. It is defined as⁵

$$\sigma = P / \rho_0 c S \langle v^2 \rangle \quad (6)$$

where P is the acoustic power radiated from the structure, $\rho_0 c$ the characteristic impedance of the air, S the surface area, and $\langle v^2 \rangle$ the spatially averaged mean-square velocity on the radiating surface.

The radiation efficiency of the modes resonant in a frequency band of interest varies as follows.

1) The radiation efficiency is unity for a frequency band that includes solely acoustically fast modes.

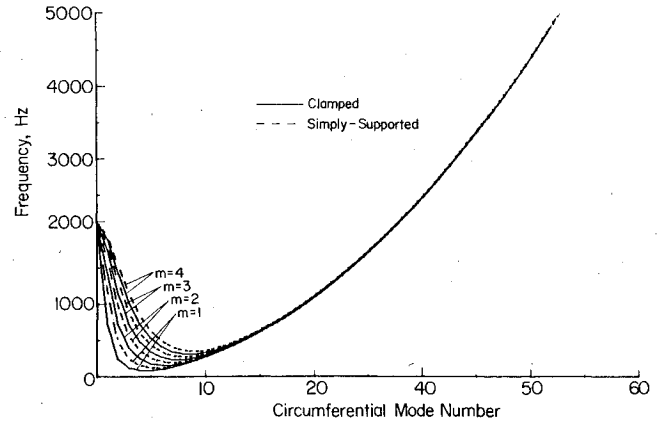


Fig. 1 Natural frequencies of a simply-supported cylinder (---) and a clamped-clamped cylinder (—).

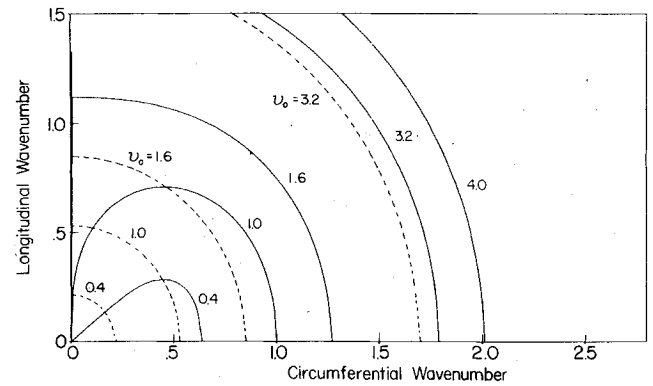


Fig. 2 Wavenumber diagram; — structural waves, --- acoustic waves.

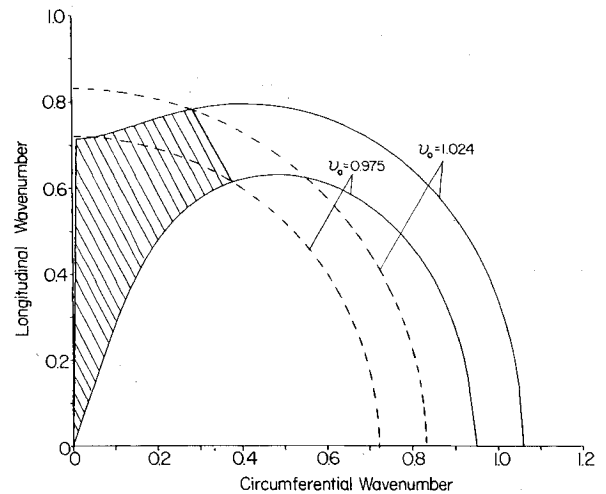


Fig. 3 Frequency band consisting of some acoustically fast modes and some acoustically slow modes; — structural waves, --- acoustical waves; shaded area includes acoustically fast modes.

2) For a band that has both acoustically fast and slow modes, the radiation efficiency may be assumed to be given approximately by the ratio of the number of acoustically fast modes to the total number of modes resonant in that band.

3) For a band that has exclusively acoustically slow modes, the radiation efficiency for those modes (circumferential edge modes of the cylinder) is given by⁴

$$\sigma = \frac{(hR)^{1/2} \left[\ln \frac{1 + (f/f_c)^{1/2}}{1 - (f/f_c)^{1/2}} + \frac{2(f/f_c)^{1/2}}{1 - f/f_c} \right]}{\pi L [12(1-\mu^2)]^{1/4} (k_a^2 + k_c^2)^{1/2} (1 - f/f_c)^{1/2}} \quad (7)$$

where f is the center frequency of the band and f_c the critical coincidence frequency. Previous studies on the radiation of sound from cylindrical shells such as the work of Manning et al.⁶ and Szechenyi⁷ utilized some approximations in obtaining the wavenumber diagrams, whereas in the work reported here, a series of computer programs has been developed to calculate the modal densities and the radiation efficiencies from the wavenumber diagrams. The present results are believed to be more accurate since the approximations made in earlier work have been avoided.⁸

Transmission Loss of a Cylindrical Shell

The sound transmission loss is defined as:

$$TL = 10 \log \left[\frac{\text{Incident acoustic power}}{\text{Transmitted acoustic power}} \right] \quad (8)$$

The transmission through a finite-length cylindrical shell can be theoretically divided into two parts, namely, the resonant transmission and the nonresonant transmission. The resonant transmission loss, TL_{res} , can be derived from the power balance equations⁴

$$TL_{\text{res}} = 10 \log \left[\frac{\omega_0^2 MS^2 (2R_{\text{rad}} + R_{\text{mech}})}{8\pi^2 c^2 n(\omega_0) R_{\text{rad}}^2} \right] \quad (9)$$

where R_{rad} is the average radiation resistance of all the modes resonant in the band under consideration, $n(\omega_0)$ the modal density in modes/Hz, R_{mech} the mechanical resistance, M the mass per unit surface area, and ω_0 the angular center frequency (of the band). The nonresonant vibration can be much more important at frequencies where the structural resonant radiation properties are weak. These nonresonant modes of a cylindrical shell can be classified into mass-controlled modes and stiffness-controlled modes below the ring frequency because of the curvature effect. This is different from the case of a flat panel where the mass and stiffness controlled regions are easily separated by the critical coincidence frequency.^{9,10} The nonresonant transmission loss of a cylinder TL_{nr} is given by two equations for the two frequency regions⁴

$$TL_{\text{nr}} = 8.33 \log \{ [\nu_0^2 (h/R)^2 E \rho_m / 4 \rho_0^2 c^2] [1 - (\nu_0 f_r / f_c)^2]^2 + 2.3 \} - 3 + 20 \log (\pi / 2 \sin^{-1} \{ \nu_0 [1 - (\nu_0 f_r / f_c)^2]^{1/2} \}^{1/2}) \quad (10)$$

for $\nu_0 \leq 1$ (below ring frequency)

$$TL_{\text{nr}} = 8.33 \log \{ [\nu_0^2 (h/R)^2 E \rho_m / 4 \rho_0^2 c^2] \times [1 - (\nu_0 f_r / f_c)^2]^2 + 2.3 \} - 3 \quad (11)$$

for $\nu_0 > 1$, (above ring frequency).

The total transmission loss of the cylinder subject to a diffuse incident sound field can be calculated from the energy sum of the resonant and the nonresonant transmission. The transmission loss thus obtained theoretically vs frequency is shown in Fig. 9 as a solid line.

III. Experimental Measurements

To rate the sound transmission property of a cylindrical shell, the difference between the incident intensity level and the transmitted intensity level is desired.¹¹

Radiation Efficiency of a Cylindrical Shell

As discussed in the previous section on radiation efficiency, the radiation efficiency of the cylinder can be determined by measuring the surface velocity of the vibrating structure and

the sound power it radiates. In this paper we have presented results of the measurement of the radiation efficiency of the cylinder under investigation. The cylinder was excited by an airborne noise source. The spatially averaged velocity was taken at 60 randomly distributed locations over the cylindrical shell. Simultaneously, the sound power radiated was evaluated from the intensity measurement made by the two-microphone acoustic intensity technique. Figure 4 presents the one-third octave band plot of the radiation efficiency measured over a frequency range of 50-10,000 Hz. Also shown in the figure are the theoretical results of the radiation efficiency obtained from the wavenumber diagrams.

The details of the procedure and the theory behind it are presented in Ref. 8. The agreement between the theoretical and experimental results seems to be fairly good—especially since the two peaks, one at the critical coincidence frequency and the other at the ring frequency, can be seen in the radiation efficiency experimental measurements.

Transmission Loss Evaluation by Acoustic Intensity Technique

A cylindrical shell of 0.76-m diameter and 1.67-m length was built by rolling 1.6-mm thick sheet steel and welding it at the joint. The boundary conditions of the cylindrical shell were intended to be fully clamped at the two ends of the shell and both ends were closed with end plates. A 15-W double-coned loudspeaker was mounted inside on brackets 0.15 m away from one end plate and was mounted eccentrically on it. The cylinder was suspended from the ceiling in an anechoic chamber with two chains as shown in Fig. 5. A steady sound field was produced inside the cylinder, by driving the loudspeaker with a random noise generator through an amplifier.

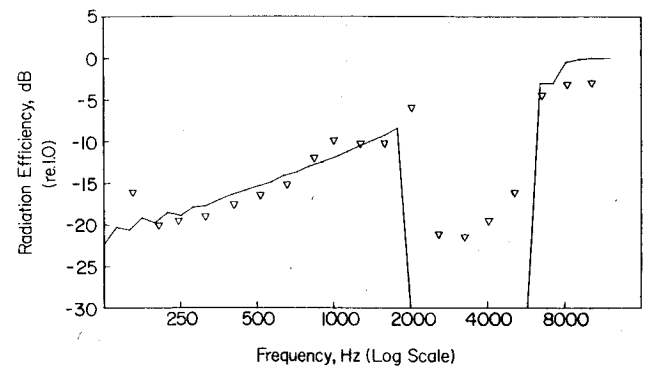


Fig. 4 Experimental results of radiation efficiency at one-third octave center frequencies (▽) compared to theoretically predicted values of radiation efficiency (—).

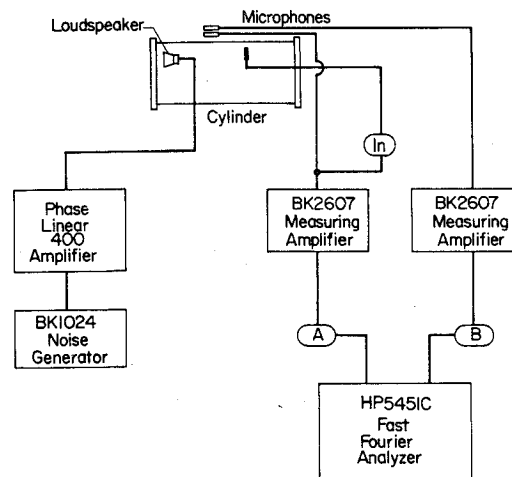


Fig. 5 Schematic diagram of the experimental set-up for the measurement of transmission loss of a cylinder.

The incident intensity was evaluated from $p_{rms}^2/4\rho_0c$ assuming the interior sound field to be diffuse. The average sound pressure inside the cylinder p_{rms} was measured by moving a microphone probe longitudinally and circumferentially inside the cylinder. The transmitted intensity through the cylinder was measured using the acoustic intensity technique.¹² The method is based on the evaluation of the cross-spectral density of the pressure signals from two closely spaced microphones. The details of the technique and its application to the evaluation of transmission loss of structures are given in Refs. 12 and 13. A spatial average was obtained by moving the two-microphone array over the entire surface area of the cylinder. Figure 6 shows the spatially-averaged narrow-band plot of the (assumed) diffuse field intensity inside the cylinder, whereas Fig. 7 shows the spatially-averaged transmitted intensity obtained by the two-microphone technique. The transmission

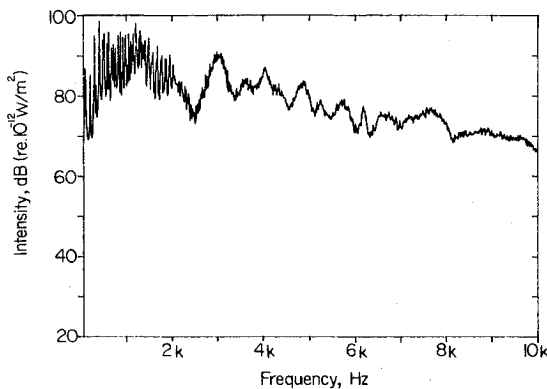


Fig. 6 Intensity incident on the cylindrical shell calculated from the sound pressure measured with a single microphone and assuming the diffuse field intensity ($p^2/4\rho_0c$).

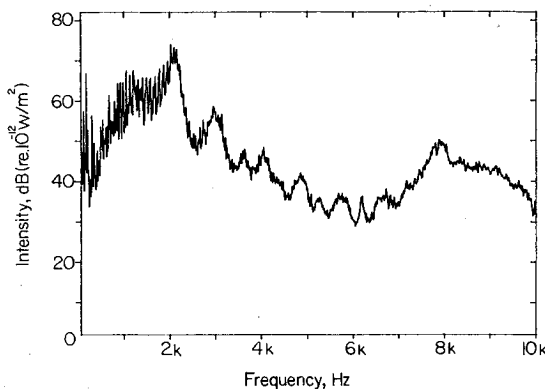


Fig. 7 Intensity transmitted through the cylindrical shell measured by the two-microphone acoustic intensity method.

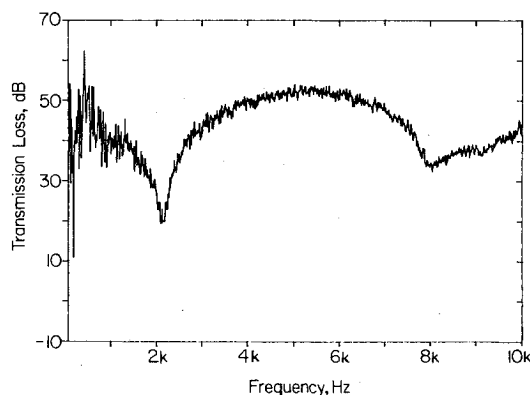


Fig. 8 Transmission loss of cylindrical shell obtained from Figs. 6 and 7.

loss of the cylindrical shell, obtained from computing 10 times the common logarithm of the ratio of the incident and transmitted sound power, is shown in Fig. 8. A one-third octave average of the results is shown in Fig. 9. Also shown in Fig. 9 is the theoretical prediction (continuous curve) of the transmission loss of the cylinder obtained from the SEA model. The experimental results agree fairly well with the theoretical prediction in the higher frequency region. It has been possible to predict the two dips in the transmission loss curve, one at the ring frequency (2100 Hz) and the other at the critical coincidence frequency (7500 Hz). The discrepancy between the experimental and theoretical predictions in the low-frequency range (below 500 Hz) may be explained as follows. The assumption that the sound field inside the cylinder is diffuse may not be true at low frequencies. There exist some strong standing waves in the cylinder in that frequency region. Hence, assuming $p_{rms}^2/4\rho_0c$ as the incident acoustic intensity at low frequencies may cause the inconsistency.

Transmission Loss Evaluated by Transmission Suite Method

The sound transmission loss of structures may be evaluated by the transmission suite method. Briefly, this method consists of the use of two reverberation rooms or spaces which are separated by the structure under investigation.¹⁴ The two rooms are called the transmission and reception rooms or spaces. The sound pressure levels in the "transmission room" and the "reception room" are measured simultaneously. The difference between these two sound pressure levels is called the noise reduction (NR). The reverberation time T_R of the reception room is also required to obtain the transmission loss TL from the noise reduction measurement, using the expression

$$TL = NR + 10 \log \left[\frac{ScT_R}{24V_2 \ln(10)} \right] \quad (12)$$

where V_2 is the volume of the reception room, and the other terms in the equation are the same as in Eq. (6).

To measure the transmission loss of the cylinder by this method a set-up similar to that discussed in the previous section was installed in a reverberation room. Again, a microphone probe was used to measure the spatially-averaged sound pressure level inside the cylinder. The average sound pressure level in the reverberation room was measured by a rotating microphone boom. The reverberation time of the reverberation room was measured for each one-third octave band center frequency. From Eq. (12), the transmission loss of the cylindrical shell was calculated and plotted in Fig. 10. A comparison of this plot with the transmission loss measurements made by the two-microphone acoustic intensity technique, which is plotted as a solid line in Fig. 10, shows that the results obtained by the two methods agree very well for frequencies above 500 Hz. In the transmission suite

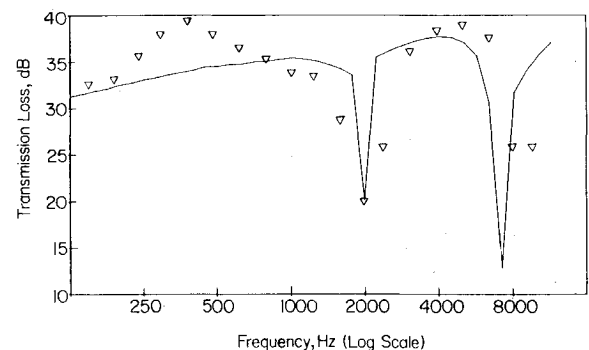


Fig. 9 Experimental results for transmission loss at one-third octave center frequencies (∇) compared to the theoretically predicted transmission loss (—).

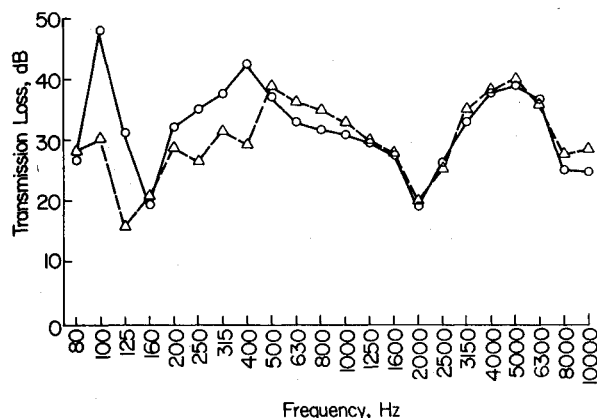


Fig. 10 Transmission loss of cylindrical shell measured by the transmission suite method (\triangle) and the acoustic intensity method (\circ).

method it is assumed that the sound fields on the incident and transmitted sides of the structure are diffuse in nature. The assumption that the field inside the cylinder is diffuse in the present case cannot be satisfied in the low-frequency range. This may explain the disagreement at low frequencies.

Discussion

The main advantage of the acoustic intensity technique to obtain the transmission loss of structures is its simplicity and accuracy. In the transmission suite method, two reverberation rooms are required, whereas in this intensity technique only one reverberation room is needed. In addition, this method is found to be more accurate than the transmission suite method as corrections are not needed for the surface area of the structure and the absorption in the receiving room.

Another important advantage of this method is that it can be used to evaluate the sound power transmitted through different parts of a composite structure which is not possible using the transmission suite method.¹³

As explained in the previous two sections, it is not easy to create a diffuse sound field in the low-frequency region inside the cylinder. An alternative way of measurement is to generate the sound field outside the cylinder in a reverberation room and then to measure the transmitted sound intensity or sound level inside the cylinder. In order to use the transmission suite method to determine the transmission loss from outside to inside, it would be necessary to obtain the reverberation time of the cylinder interior volume which would probably be quite difficult. However, using the two-microphone acoustic intensity method to determine the transmission loss from outside to inside, it is not necessary to determine the interior reverberation time and this approach will be discussed in Sec. IV.

IV. Comparison of Different Methods of Measuring Transmission Loss of a Cylinder

As just discussed, an alternative method to measure the transmission loss was investigated by suspending the cylinder in a reverberation room. A very intense sound field was generated in the reverberation room by the use of a random noise generator, amplifier, and loudspeaker combination. The central interior of the cylinder was filled with a large amount of 48 kg/m³ (3.0 lb/ft³) wedge-shaped pieces of fiberglass to make the interior sound field as anechoic as possible. A bracket holding the two microphones was mounted on the centerline of the cylinder. The two microphones were held so that the line joining their centers was in the radial direction and the microphone closer to the shell was 10 mm away from the surface. During the measurement the microphones were rotated circumferentially along the cylindrical shell to obtain a spatially-averaged sound intensity.

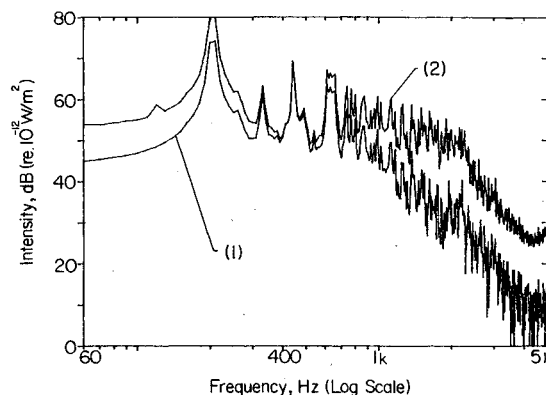


Fig. 11 Space-averaged sound intensity in the bare cylinder interior; (1) two-microphone acoustic intensity measurement compared with (2) free-field intensity calculation ($p^2/\rho_0 c$).

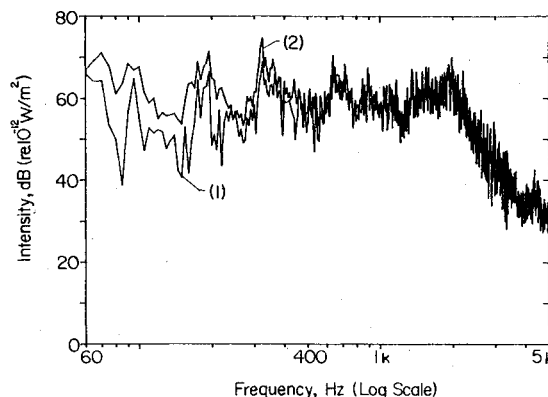


Fig. 12 Space-averaged sound intensity in the cylinder interior with the fiberglass wedges installed; (1) two-microphone acoustic intensity measurement compared with (2) free-field calculation ($p^2/\rho_0 c$).

Sound Field Inside the Cylinder

In order to check on the values of intensity transmitted through the cylinder, the transmitted intensity obtained from the two-microphone method was compared with that calculated from the free-field intensity result ($p_{rms}^2/\rho_0 c$). Initially the measurement was made in the interior of the cylinder, without installing any fiberglass. Figure 11 shows a comparison of the intensity obtained from the two-microphone method with that from the free-field intensity. Due to reflections from all directions, the sound field is more like a diffuse field. When the fiberglass wedges were installed, the sound field became much closer to that predicted by the free-field results. The interior intensity obtained from the two-microphone technique now agrees very well with that of the free-field intensity ($p_{rms}^2/\rho_0 c$) obtained from a single microphone measurement. This is shown in Fig. 12.

Transmission Loss Measured with Exterior Noise Source

As explained before, the intensity transmitted through the cylindrical shell was measured using two closely spaced microphones installed inside the cylinder. The incident intensity in this case was measured by a single microphone mounted on a rotating boom in the reverberation room. Figure 13 shows narrow-band plots of the transmission loss of the cylindrical shell as obtained in the two cases studied; 1) with the noise source in the cylinder and the transmitted intensity measured on the exterior surface of the cylinder when it was situated in an anechoic room and 2) with the noise source outside the cylinder when it was situated in a reverberation room and the transmitted intensity measured on the interior surface of the cylinder which was filled with fiberglass and thus anechoic inside. Good agreement is found between the two plots in the high-frequency region above 1500 Hz.

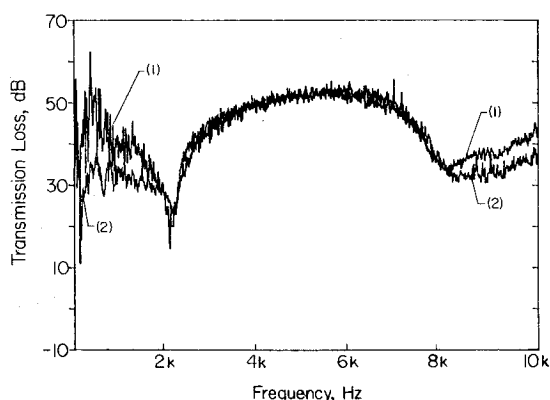


Fig. 13 Transmission loss of the cylindrical shell measured by two-microphone acoustic intensity method in (1) outward and (2) inward directions.

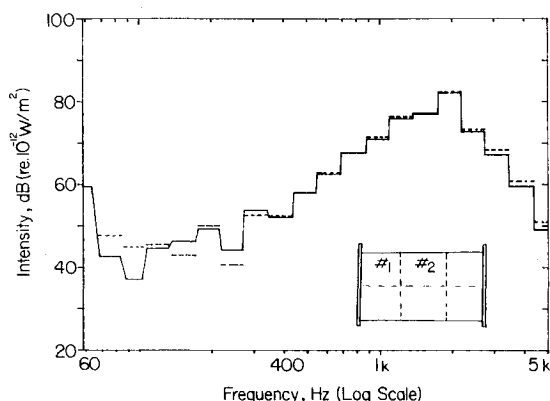


Fig. 14 Space-averaged sound intensity radiated from different sections of a cylindrical shell: - - - section 1, — section 2.

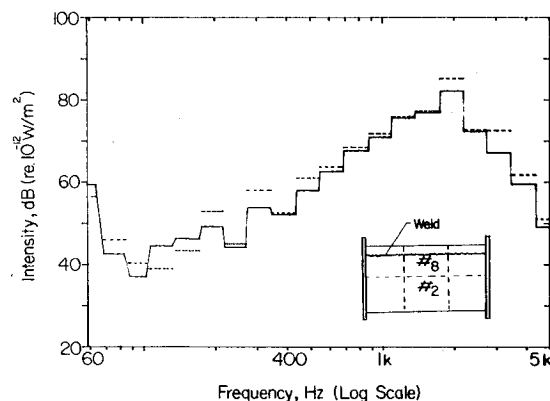


Fig. 15 Space-averaged sound intensity radiated from different sections of a cylindrical shell: - - - section 2, — section 8.

Discussion

In order to generate a diffuse sound field, two basic conditions are required, namely, high modal density and low cavity absorption. It has been found easier to create a diffuse field in the low-frequency range in the reverberant room than in the interior volume of the cylinder because the modal density is higher in the former case. On the other hand, Fig. 12 shows that the interior volume of the cylinder is reasonably anechoic when the fiberglass wedges are installed. Hence, it is believed that the transmission loss determined from the transmitted intensity measured in the interior volume of the cylinder when it was made internally anechoic and was subjected to an external diffuse incident field is more accurate than the transmission loss values obtained when the sound

source was placed in the cylinder and intensity measurements were made on the exterior surface of the cylinder which was situated in an anechoic room. This is especially true in the low-frequency region.

The agreement between the transmission loss measurements when the noise source is either in the cylinder or exterior to it in the high-frequency region also indicates that measurements can be done in either direction on a real aircraft fuselage providing that the incident field is diffuse and the receiving space is anechoic for both situations. For example, if only an anechoic chamber is available, one can use an interior sound source and measure the transmitted intensity with the two-microphone method outside the fuselage, even though the real aircraft has noise sources outside the cabin.

The authors have recently continued their work by using the two microphone method to measure the transmission loss of different parts of a real aircraft fuselage. This work is reported in Ref. 15.

V. Effect of Structural Joints and Source Positions on Transmission Measurement

The sound intensity transmitted through the cylinder was measured by the two-microphone technique on the exterior surface of the cylinder. It is of interest to compare the sound radiated from different sections of the cylinder surface area. The effect of the clamped edges of the cylinder on the sound power radiated by the cylinder is presented in Fig. 14. Area 1 has one edge clamped by two rings while area 2 is not clamped along any edge. From the figure, the transmitted intensity seems to be little affected by boundaries. Next a comparison of the intensity transmitted from the sections with and without a welding joint was made. The area 8 which includes a welding joint seems to radiate less power than the area 2 which is without a welding joint. This comparison is illustrated in Fig. 15.

VI. Conclusions

The measured transmission loss results obtained by using the new two-microphone acoustic intensity technique compared well with the transmission loss prediction made by statistical energy analysis (SEA). It has been possible to predict both, theoretically and experimentally the first dip at the ring frequency and the other at the critical coincidence frequency in the transmission loss curve of the cylinder as shown in Figs. 8 and 9. The experimental results also seem to compare well with the transmission loss measured by the conventional transmission suite method in the higher frequency range.

The two-microphone acoustic intensity method was also used to investigate the nature of the sound transmission through a cylindrical shell, when the noise source was in the interior of the cylinder, or when it was outside the cylinder, when the incident sound field was diffuse and the receiving space was anechoic in both cases. Very good agreement was obtained for the transmission loss of the cylinder measured in the two cases, in the high frequency region.

Acknowledgment

The authors would like to thank NASA, Hampton, Virginia for financial support under Grant number NAG-1-58.

References

- Love, A.E.N., "On the Small Free Vibrations and Deformations of Thin Elastic Shells," *Philosophical Transactions of the Royal Society (London)*, Vol. 179A, 1888, pp. 491-546.
- Soedel, W., *Vibrations of Shells and Plates*, Marcel Dekker Inc., New York, 1981, pp. 135-143.

³Soedel, W., "A New Frequency Formula for Closed Circular Cylindrical Shells for a Large Variety of Boundary Conditions," *Journal of Sound and Vibration*, Vol. 70, No. 3, 1980, pp. 309-317.

⁴Szechenyi, E., "Sound Transmission Through Cylinder Walls Using Statistical Considerations," *Journal of Sound and Vibration*, Vol. 19, No. 1, 1971, pp. 83-94.

⁵Cremer, L., Heckl, M., and Ungar, E. E., *Structure-Borne Sound*, Springer-Verlag, 1973, pp. 455-465.

⁶Manning, J. E. and Maidanik, G., "Radiation Properties of Cylindrical Shells," *Journal of the Acoustical Society of America*, Vol. 36, No. 9, 1964, pp. 1691-1698.

⁷Szechenyi, E., "Modal Densities and Radiation Efficiencies of Unstiffened Cylinders Using Statistical Methods," *Journal of Sound and Vibration*, Vol. 19, No. 1, 1971, pp. 65-81.

⁸Forssen, B., Wang, Y. S., Raju, P. K., and Crocker, M. J., "Study of Methods to Predict and Measure the Transmission of Sound Through Walls of Light Aircraft," Herrick Laboratories, Purdue University, Rept. 81-19, Aug. 1981.

⁹Lyon, R. H., *Statistical Energy Analysis of Dynamic Systems*, MIT Press, 1975, Chap. 12.

¹⁰Szechenyi, E., "Formulae for the Non-Resonant Transmission of Diffuse Sound Through Stiff Walls," Institute of Sound and Vibration Research Tech. Rept. 39, University of Southampton, 1970.

¹¹Crocker, M. J. and Price, A. J., "Sound Transmission Using Statistical Energy Analysis," *Journal of Sound and Vibration*, Vol. 9, No. 3, 1969, pp. 469-486.

¹²Crocker, M. J., Forssen, B., Raju, P. K., and Mielnicka, A., "Measurement of Transmission Loss of Panels by Acoustic Intensity Technique," *Proceedings, Inter-Noise 80*, 1980, pp. 741-746.

¹³Crocker, M. J., Raju, P. K., and Forssen, B., "Measurement of Transmission Loss of Panels by the Direct Determination of Transmitted Acoustic Intensity," *Noise Control Engineering*, Vol. 17, No. 1, 1981, pp. 6-11.

¹⁴Crocker, M. J., "The Response of Structures to Acoustic Excitation and the Transmission of Sound and Vibration," Ph.D. Thesis, The University of Liverpool, England, 1969.

¹⁵Wang, Y. S. and Crocker, M. J., "Direct Measurement of Transmission Loss of Aircraft Structures Using the Acoustic Intensity Approach," *Noise Control Engineering Journal*, Vol. 19, No. 3, 1982, pp. 80-85.

From the AIAA Progress in Astronautics and Aeronautics Series . . .

AERO-OPTICAL PHENOMENA—v. 80

Edited by Keith G. Gilbert and Leonard J. Otten, Air Force Weapons Laboratory

This volume is devoted to a systematic examination of the scientific and practical problems that can arise in adapting the new technology of laser beam transmission within the atmosphere to such uses as laser radar, laser beam communications, laser weaponry, and the developing fields of meteorological probing and laser energy transmission, among others. The articles in this book were prepared by specialists in universities, industry, and government laboratories, both military and civilian, and represent an up-to-date survey of the field.

The physical problems encountered in such seemingly straightforward applications of laser beam transmission have turned out to be unusually complex. A high intensity radiation beam traversing the atmosphere causes heat-up and breakdown of the air, changing its optical properties along the path, so that the process becomes a nonsteady interactive one. Should the path of the beam include atmospheric turbulence, the resulting nonsteady degradation obviously would affect its reception adversely. An airborne laser system unavoidably requires the beam to traverse a boundary layer or a wake, with complex consequences. These and other effects are examined theoretically and experimentally in this volume.

In each case, whereas the phenomenon of beam degradation constitutes a difficulty for the engineer, it presents the scientist with a novel experimental opportunity for meteorological or physical research and thus becomes a fruitful nuisance!

412 pp., 6 × 9, illus., \$30.00 Mem., \$45.00 List

TO ORDER WRITE: Publications Dept., AIAA, 555 West 57th Street, New York, N.Y. 10019